SYNTHESIS AND OPTICAL PROPERTIES OF Mn-DOPED PbTiO$_3$ NANOPOWDERS BY MICROWAVE ASSISTED SOL-GEL METHOD

Romteera Chueachot[a,b], Sert Kiennork[b], Pakawat Wongwanwattana[b], Ronariddh Nakhowong[b,c,]*

[a]*Program of Chemistry, Faculty of Science, Ubon Ratchathani Rajabhat University, Ubon Ratchathani, 34000, Thailand*
[b]*Program of Physics, Faculty of Science, Ubon Ratchathani Rajabhat University, Ubon Ratchathani, 34000, Thailand*
[c]*Functional Nanomaterials and Electrospinning Research Laboratory, Faculty of Science, Ubon Ratchathani Rajabhat University, Ubon Ratchathani, 34000, Thailand*

ABSTRACT

In this work, Mn-doped PbTiO$_3$ (Mn$_x$Pb$_{1-x}$TiO$_3$, x = 0, 0.01, 0.05, and 0.10) nanopowders were successfully synthesized by microwave assisted sol-gel method. The nanopowders were treated with microwave power of 300 W for 5 min and then, calcined at 700 °C for 4 h in air. The X-ray diffraction results confirmed that the crystalline phases correspond to PbTiO$_3$ and small amount of rutile-TiO$_2$ were detected. The scanning electron microscopy and transmission electron microscopy images revealed that Mn$_x$Pb$_{1-x}$TiO$_3$ nanopowders exhibits agglomerate particles with elliptical and spherical-like shapes and the grain size of approximately 200–400 nm. The band gap energy of the samples was found to be 2.6–3.10 eV. Fourier transform infrared spectroscopy spectra showed that the absorption bands are in range of 500-700 cm^{-1}, indicating the formation of metal oxide.

*
Corresponding authors; e-mail: ro_phy110@hotmail.com, Tel: +66-4535-2000

INTRODUCTION

Recently, the structured nanomaterials, including nanoparticles, nanorods, nanotubes, and nanofibers have been extensively investigated due to its a high surface to volume ratio, small pore size, and chemical stability over the bulk materials [1]. The unique property of nanomaterials with different morphologies has benefits to applications in solar cells, supercapacitors, Li-ion batteries, fuel cell, and other [2]. Lead titanate (PbTiO$_3$) with perovskite structure has an important material for its remarkable ferroelectricity, piezoelectricity, pyroelectricity, and colossal magnetoresistivity, and its application in optoelectronics, transducers, sensors and non-volatile memories which makes much attraction for applications in various fields [3]. For the piezoelectric properties, PbTiO$_3$ changes from a tetragonal to a cubic structure phase or change from ferroelectric to paraelectric transition at the Curie temperature T_c~494 °C [4]. Manganese as dopant can improves charge separation between electron and hole by forming electron traps and enhances the photocatalytic activity [5]. Moreover, Mn dopant exhibit increasing light absorption capacity of the doped materials. Recently, the PbTiO$_3$ were successfully synthesized by various techniques such as sol-gel method [3], solid state reaction [6], electrospinning [7], and hydrothermal method [8]. The microwave-assisted synthesis has attracted widespread as a novel heating model in materials science due to its advantage of being faster, simple, rapid heating, low reaction temperature, high growth rates, high quality of nanostructures, and low energy requirement [9]. The benefit of microwave irradiation is due to ultra-fast and uniform solution warm up to the crystallization temperatures [10]. In this work, we report the effect of Mn-doped PbTiO$_3$ by microwave assisted sol-gel method at different Mn content. The structural, morphology and optical properties of the samples were investigated using X-ray diffraction, UV-vis diffuse reflectance spectroscopy, scanning electron microscopy, transmission electron microscopy,

and Fourier transform infrared spectroscopy under different amount quantities of Mn doping.

MATERIALS AND METHODS

$Mn_xPb_{1-x}TiO_3$ (x = 0, 0.01, 0.05 and 0.10) were prepared by microwave assisted sol-gel method. Firstly, different quantities of lead(II) acetate trihydrate ($Pb(CH_3CO_2)_2 \cdot 3H_2O$, QREC) and manganese (II) acetate tetrahydrate ($Mn(CH_3COO)_2 \cdot 4H_2O$, Aldrich) with stoichiometry were dissolved in mixture solution of 5 mL glacial acetic acid (CH_3COOH, Acros Organics) and 40 mL ethanol and magnetic stirred at ambient temperature for 1 h.Then, 10 mmol of titanium (IV) isopropoxide (TTIP, $Ti[OCH(CH_3)_2]_4$, Aldrich) was dissolved in 2 rmL acetic acid and 10 mL ethanol and magnetic stirring. Subsequently, TTIP solution were added drop by drop to above solution while continuous stirring for 8 h to obtain a mixture solution. The solution was treated with domestic microwave oven (ME712N model, SAMSUNG) at microwave power of 300 W for 5 min and then, annealing at 120 °C for 4 h to remove the volatile solvents. The dried precursor was calcined at 300 °C for 8 h to remove the organic compounds. The dried powders were grinded and calcined at 700 °C for 4 h. For the comparison, $Mn_{0.10}Pb_{0.90}TiO_3$ was prepared by the same method without the microwave treatment.

The crystalline phases of the samples were determined with an X-ray diffraction (XRD, Phillips, X'Pert MPD) using CuKα radiation (λ=1.5406 Å). The surface morphology of the samples was observed by transmission electron microscopy (TEM, JEM-2010, JEOL) and scanning electron microscopy (SEM, JSM-5410LV, JEOL) attached with energy-dispersive X-ray spectroscopy (EDS). UV-vis diffuse reflectance spectra were carried out using UV-vis spectrophotometer (T90+, PG instrument) attached with integrating sphere at ranging from 230–850 nm using $BaSO_4$ as reference. The functional groups of samples were recorded by Fourier transform infrared spectrometer (FT-IR, Spectrum RX1, Perkin Elmer Ltd.).

RESULTS AND DISCUSSION

The crystalline phases of $Mn_xPb_{1-x}TiO_3$ nanopowders are presented in Fig. 1. The XRD patterns showed that the diffraction peaks are in good agreement to $PbTiO_3$ [JCPDS card no: 77-2002] with tetragonal structure and small amount of rutile TiO_2 was also detected. After Mn content were doped in $PbTiO_3$ at different quantities, it was clear that the intensity of diffraction peaks decrease with increasing of Mn content. The decrease of the diffraction peak intensity indicated

the loss of crystallinity due to the lattice distortion by the incorporation of Mn content in to the $PbTiO_3$ lattice [10].
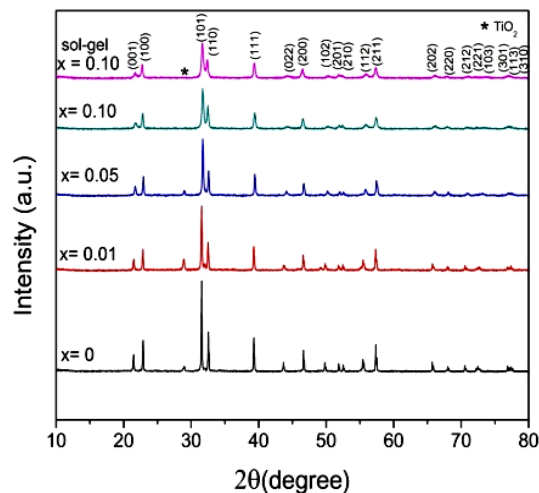
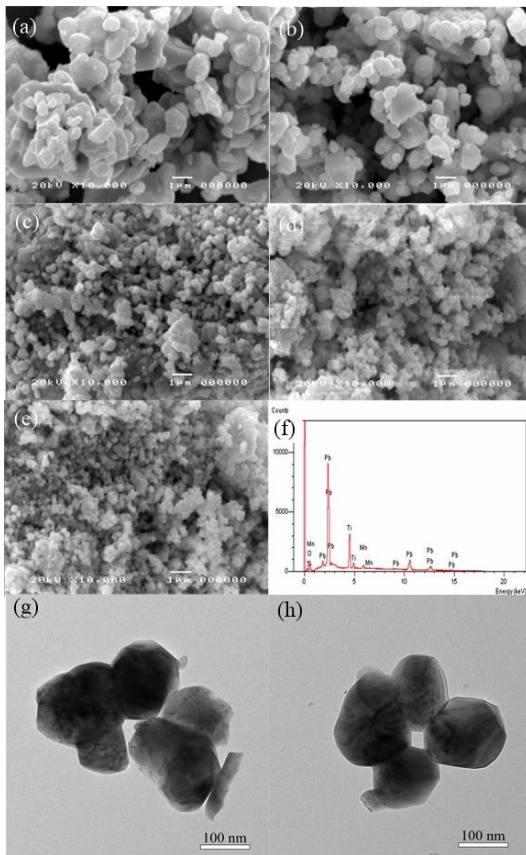**Fig. 1** XRD patterns of $Mn_xPb_{1-x}TiO_3$ nanopowders.

The average crystallite size of the samples was calculated using the Scherrer equation [11]:

$$D = \frac{0.9\lambda}{\beta \cos\theta} \qquad (1)$$

where D is average crystallite size, β is the full width at half maximum (FWHM) of the XRD peak, θ is the diffraction angle, λ and is the X-ray wavelength corresponding to CuKα radiation. The crystallite size of the sample was found to be 117.93, 103.19, 91.76, and 51.61 nm at x = 0, 0.01, 0.05, and 0.10, respectively. For the sol-gel method, the crystallite size of $Mn_{0.10}Pb_{0.90}TiO_3$ is about 55.61 nm which is slightly different from microwave assisted sol-gel method. The crystallite size results showed that crystallite size decrease as the increasing of Mn content, indicating the Mn-doped $PbTiO_3$ can prevent the growth of crystal due to Mn content at the Pb sites in $PbTiO_3$ structure [12].

The SEM images of pure and Mn-doped $PbTiO_3$ nanopowers shown in Fig. 2. It is clearly evident that the pure $PbTiO_3$ nanopowders consist of agglomerated particles with elliptical and spherical-like shapes. The average particle size is about 985±335 nm. After Mn content increased, the particle size became decreases as Mn content increase with particle size approximately 670±173, 280 ±65, 238±43 nm at x = 0.01, 0.05, 0.10, respectively. However, the particle size of sol-gel method reveal that the particle size is about 275±49 nm at x = 0.10, which is slightly different from microwave assisted sol-gel method.

Fig. 2 SEM images of $Mn_xPb_{1-x}TiO_3$ nanopowders at (a) x = 0, (b) x= 0.01, (c) x = 0.05, (d) x = 0.10, (e) x = 0.10; sol-gel method, (f) EDS spectrum (x=0.10, microwave assisted sol-gel method), (g) typical TEM images of the sol-gel method, and (h) microwave assisted sol-gel method of $Mn_{0.10}Pb_{0.90}TiO_3$ nanopowders.

The SEM image results revealed that grain size decrease as the increasing Mn content. The EDS spectrum (Fig. 2(g and h)) confirms the presence of Mn, Pb, Ti, and O elements exist in the samples without any impurity. The TEM images (Fig. 2(g and h)) evident that the grain size of Mn doped $PbTiO_3$ (x=0.10) found to be 135 and 128 nm after untreated and treated with microwave irradiation, respectively.

UV-vis diffuse reflectance spectra (Fig. 3a) shows highest absorption increase in the UV and visible light region ranging from 250 to 600 nm after Mn content increasing. The bands in the region of 400–600 nm confirm the presence of Mn cations and the increase of Mn amount in the $PbTiO_3$ lattice [12].
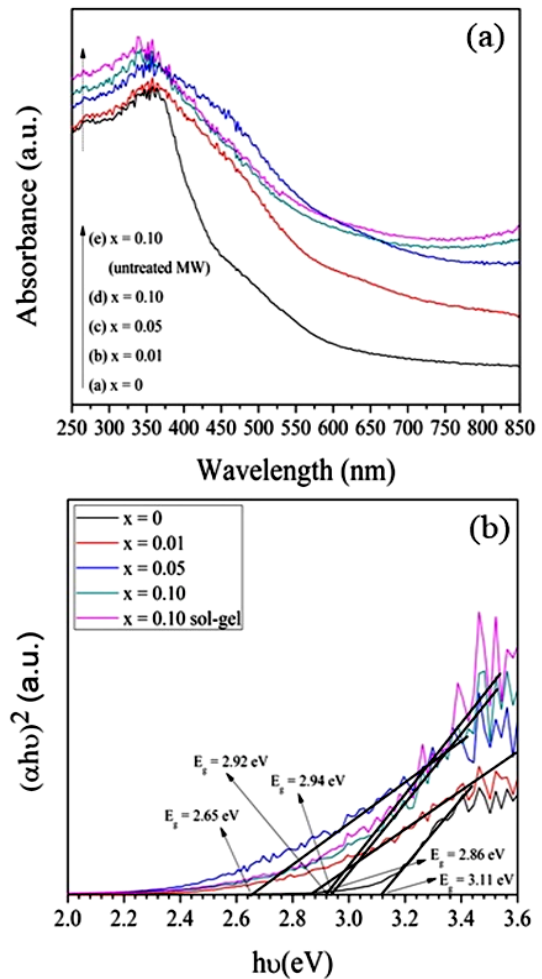
Fig. 3 UV-vis diffuse reflectance spectra of (a) absorption, and (b) plot of $(\alpha h\nu)^2$ versus $h\nu$.

The increase of absorption in the UV light region can be related to a structural modification due to the insertion of Mn cations into the $PbTiO_3$ lattice. The band gap energy could be derived using the formula [13]:

$$\alpha h\nu = A(h\nu - E_g)^{n/2} \qquad (2)$$

where E_g is the band gap energy, α is the absorption coefficient, A is the proportionality constant, $h\nu$ is the photon energy and n can take the vulues of 1/2, 3/2, 2 or 3, when transition are direct allowed, direct forbidden, indirect allowed and indirect forbidden, respectively. The $PbTiO_3$ is indirect semiconductor (n = 4 was adopted), the band gap energies of the samples were found tobe 3.11, 2.86, 2.60, and 2.94 eV at x = 0, 0.01, 0.05, and 0.10 respectively. The sol-gel method with Mn content at x = 0.10, the ban gap energy is about 2.92 eV, which is slightly different from microwave assisted sol-gel method. The different

band gap energy is due to various factors such as quantum confinement effect, particle size, preparation method, etc[14]. However, Mn-doped $PbTiO_3$ can be decrease the band gap energy of pure $PbTiO_3$ expands to visible light region, which are wide applications in photocatalytic activity, solar cell and other.

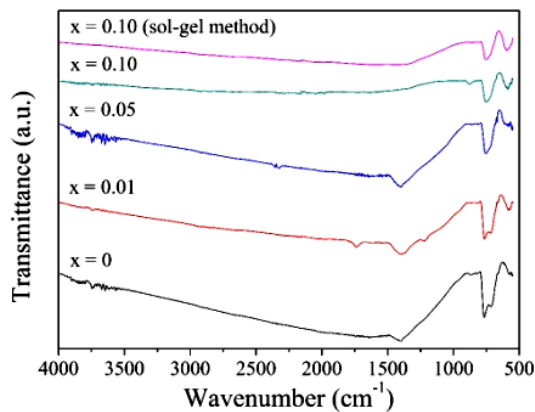**Fig. 4** FT-IR spectra of $Mn_xPb_{1-x}TiO_3$ nanopowders

FT-IR spectra of pure and Mn-doped $PbTiO_3$ nanopowders are shown in Fig.4. It was seen that a strong absorption bands at $500 - 800$ cm^{-1} are assigned to the stretching and vibration modes of metal and oxygen bonds in the samples. The peaks in range of 690–770 cm-1are ascribed to stretching vibration of metal and oxygen of $PbTiO_3$. The decreasing of the peak at 1400 cm^{-1} was due to increasing of Mn dopant and decreasing of the crystallite sizes. After Mn content was doped to $PbTiO_3$, the characteristic peak gradually appears at about 580 cm^{-1} due to stretching vibration of Mn-O bonds [15].

CONCLUSION

Mn-doped $PbTiO_3$ nanopowders were successfully prepared using microwave assisted sol-gel method. The XRD and FT-IR results confirm the crystalline phases are agreement to $PbTiO_3$. The SEM and TEM images showed the ellipsoid and spheroid-like shapes. The results revealed that the presence of Mn cations in $PbTiO_3$ lattice can improve the crystallinity, morphology, optical properties, which can be wide application in the electronic devices.

ACKNOWLEDGEMENTS

This invited article was presented at the 4th Southeast Asia Conference on Thermoelectrics, Danang, Vietnam during December 15–18, 2016.

REFERENCES

[1] S.V. Kuchibhatla, A.S. Karakot, D. Bera, S. Seal, One dimensional nanostructured materials, Prog. Mater Sci. 52 (2007) 699–913.

[2] Z. Dong, S.J. Kennedy, W. Yiquan, Electrospinning materials for energy-related applications and devices, J. Power Sources. 196 (2011) 4886–4904.

[3] S.D. Cheng, C.H. Kam, Y. Zhou, W.X. Que, Y.L. Lam, Y.C. Chan, Sol gel derived nanocrystalline thin films of $PbTiO_3$ on glass substrate, Thin Solid Films. 375 (2000) 109–113.

[4] X. Zhiguo, W. Haidou, X. Binshi, M. Guozheng, H. Yanfei, K. Jiajie, Structural integrity and ferroelectric–piezoelectric properties of $PbTiO_3$ coating prepared via supersonic plasma spraying, Mater. Des. 62 (2014) 57–63.

[5] Ş.Ş Türkyılmaz, N. Güy, M. Özacar, Photocatalytic efficiencies of Ni, Mn, Fe and Ag doped ZnO nanostructures synthesized by hydrothermal method: The synergistic/antagonistic effect between ZnO and metals, J. Photochem. Photobiol., A. 341 (2017) 39–50.

[6] V. Stankus, J. Dudonis, Lead titanate thin film synthesis by solid-state reactions, Mater. Sci. Eng., B. 109 (2004) 178–182.

[7] A. Singh, V. Gupta, K. Sreenivas, R.S. Katiyar, Influence of Ca additives on the optical and dielectric studies of sol–gel derived $PbTiO_3$ ceramics, J. Phys. Chem. Solids. 68(2) (2007) 119–123.

[8] Y. Li, H. Sun, N. Wang, W. Fang, Z. Li, Effects of pH and temperature on photocatalytic activity of $PbTiO_3$ synthesized by hydrothermal method, Solid State Sci. 37 (2014) 18–22.

[9] H. Mirzaei, A.Davoodnia, Microwave Assisted Sol-Gel Synthesis of MgO Nanoparticles and Their Catalytic Activity in the Synthesis of Hantzsch 1,4-Dihydropyridines, Chin. J. Catal. 33 (2012) 1502-1507

[10] R. Soleimanzadeh, M.S.S. Mousavi, A. Mehrfar, Z.K. Esfahani, M. Kolahdouz, K. Zhang, Sequential microwave-assisted ultra-fast ZnO nanorod growth on optimized sol-gel seedlayers,

J. Cryst. Growth. 426 (2015) 228−233.

[11] S. Maryam, B. Mahsa, O. Keyvan, Application of MnTiO$_3$ nanoparticles as coating layer of high performance TiO$_2$/MnTiO$_3$ dye-sensitized solar cell, J. Ind. Eng. Chem. 20(5) (2014) 3646−3648.

[12] S. Sankar, S.K. Sharma, A. Namhyun, H. Lee, D.Y. Kim, Y.B. Im, Photocatalytic properties of Mn-doped NiO spherical nanoparticles synthesized from sol-gel method, Optik.127(22) (2016) 10727−10734.

[13] R. Lopez, R. Gomez, Band-gap energy estimation from diffuse reflectance measurements on sol–gel and commercial TiO$_2$: a comparative study, J. Sol-Gel SciTechol. 61(1) (2012) 1−7.

[14] L. Gupta, A. Mansingh, P.K. Srivastava, Band gap narrowing and the band structure of tin-doped indium oxide films, Thin Solid Films. 176(1) (1989) 33–44.

[15] L. Jiyuan, B. Ling-Tao, C. Wei-Guo, C. Teng, C. Yuan-Cheng, Facile fabrication of coaxial-cable like Mn$_2$O$_3$ nanofiber by electrospinning: Application as electrode material for supercapacitor, J. Taiwan Inst. Chem. Eng. 65 (2016) 584−590.